Temperature fluctuations in a convection cell with rough upper and lower surfaces

Y.-B. Du and P. Tong*
Department of Physics, Oklahoma State University, Stillwater, Oklahoma 74078
(Received 20 July; revised manuscript received 11 October 2000; published 22 March 2001)

A turbulent convection experiment is conducted in a cell with rough upper and lower surfaces. Temperature statistics, frequency power spectrum, and thermal dissipation are measured over varying Rayleigh numbers in the central region of the cell. The temperature histogram in the rough cell is found to have the same exponential shape as that in the smooth cell, but the width of the distribution is increased by ~25%. The measured power spectrum shows that temperature fluctuations in the rough cell are increased uniformly across the whole frequency range. The cutoff frequency f_c of the power spectrum and the time averaged square temperature time derivative $\langle(\partial T/\partial t)^2\rangle$ are used to characterize the thermal dissipation in turbulent convection. It is found that the normalized f_c as well as $\langle(\partial T/\partial t)^2\rangle$ in the smooth and rough cells with different aspect ratios can all be superposed onto a single curve, indicating that the thermal dissipation in these cells is determined by the same mechanism. The experiment suggests that the enhanced heat transport observed in the rough cell is determined primarily by the local dynamics near the upper and lower boundaries.

DOI: 10.1103/PhysRevE.63.046303 PACS number(s): 47.27.Te, 05.40.−a, 44.25.+f, 47.27.Sd

I. INTRODUCTION

A main issue in the study of turbulent thermal convection is to understand whether the heat transport in turbulent convection is determined primarily by the thermal plumes that erupt from the upper and lower boundary layers or by the large-scale circulation that spans the height of the convection cell [1]. These two coherent structures are found to coexist in the convection cell and have been adopted in several theoretical models [2–4]. The experiment by Castaing and coworkers [2,5] showed that the normalized heat flux, or the Nusselt number Nu, scales as $\mathrm{Nu}\sim\mathrm{Ra}^{\gamma}$, where Ra is the Rayleigh number. The measured values of the exponent γ by various experimental groups lie in the range between 0.28 and 0.31 [1,4], which are different from the classical $\mathrm{Ra}^{1/3}$ prediction [6].

It is found that the scaling behavior of the heat transport is robust and remains unchanged under various perturbations, such as horizontal shearing of a boundary layer [7], vertical rotation of the whole convection cell [8], changes of the aspect ratio of the convection cell [9], alterations of the large-scale circulation by introducing bluff obstacles on the conducting plates [10] and sidewalls [11], and use of convecting fluids with different Prandtl numbers [12–14]. In a more recent experiment, Xu *et al.* [15] carried out high precision heat transport measurements and found deviations from the single power-law behavior.

To find the real mechanism for turbulent heat transport, we have recently carried out a convection experiment in a cell with rough upper and lower surfaces [16,17]. The measured heat transport in the rough cell is found to be increased by more than 76%. Flow visualization and near-wall temperature measurements revealed the dynamics for the emission of thermal plumes near a rough surface. The striking effect of the surface roughness provides useful insights into the roles played by the thermal plumes in determining the heat transport in turbulent convection. The discovery of enhanced heat transport over a rough surface has important applications in engineering, geography, and meteorology. An example is convection in the atmosphere and oceans, where the underlying surfaces are usually rough.

An interesting question one might ask is how the surface roughness affects the temperature fluctuations in the bulk region of the cell. Our current knowledge about the roughness effect on turbulent flows comes largely from experiments in wind tunnels and other open systems [18], in which the disturbance flow produced by a rough wall is confined in the near-wall region and is quickly discharged downstream. For these reasons the surface roughness usually does not perturb the turbulent bulk region very much, and its effect is often described by rescaling the relevant length scales with the surface roughness height [19]. The situation is changed significantly for flows in a closed cell, in which the disturbances produced by the boundaries are inevitably mixed into the bulk region.

In this paper, we report a systematic study of temperature fluctuations in the central region of the rough cell. Temperature statistics, the frequency power spectrum, and thermal dissipation are measured over varying Rayleigh numbers. The results in the rough cell are compared with those in the smooth cell. The remainder of the paper is organized as follows. We first describe the apparatus and experimental method in Sec. II. Experimental results are discussed in Sec. III. Finally, the work is summarized in Sec. IV.

II. EXPERIMENTAL METHOD

The experiment was conducted in a vertical cylindrical cell filled with water. Details of the apparatus have been described elsewhere [17] and here we only mention some key points. The sidewall of the cell was made of transparent Plexiglas with an inner diameter 19 cm and wall thickness 0.63 cm. Two Plexiglas rings with the same diameter but having two different heights, 20 cm and 40 cm, were used to extend the accessible range of the Rayleigh number. The corresponding aspect ratios $A(=\text{diameter/height})$ of the cell were $A\simeq 1.0$ and $A\simeq 0.5$.

*Email address: ptong@okstate.edu

Two identical convection cells, one with smooth upper and lower surfaces (''smooth cell'') and the other with rough upper and lower surfaces (''rough cell''), were made for comparison. The rough surface was made by regular woven V-shaped grooves with a vertex angle of 90°. The spacing between the grooves was such that a square lattice of pyramids was formed on the surface. The height of the pyramids (the roughness height) was $h=9.0$ mm. The height of the Plexiglas rings used for the rough cell was adjusted slightly, so that the base-to-base distance between the two opposing rough surfaces was the same as the height of the corresponding smooth cell.

Both the smooth and rough plates were made of brass and their surfaces were electroplated with a thin layer of gold. The lower surface of the cell was heated uniformly by two film heaters. The temperature of the upper surface was maintained constant by circulating cold water from a temperature bath. The whole convection cell was wrapped in three layers of thermal insulating rubber sheets to prevent heat leakage. The temperature of each plate was recorded by a thermistor, which was embedded near the center of plate. The control parameter of the experiment was the Rayleigh number $\mathrm{Ra}=\alpha g H^3 \Delta T/(\nu\chi)$, where H is the cell height, ΔT is the temperature difference between the upper and lower surfaces, g is the gravitational acceleration, and α, ν, and χ are, respectively, the thermal expansion coefficient, the kinematic viscosity, and the thermal diffusivity of the convecting fluid. In the experiment, the mean temperature of the bulk fluid was kept at 30 ± 1 °C and the corresponding Prandtl number $\mathrm{Pr}=\nu/\chi$ was ~5.4.

A stainless steel tube of diameter 1.1 mm was installed through the center of the upper plate to guide a small thermistor into the cell. The tube was mounted on a micrometer-controlled translation stage, such that the local fluid temperature $T(z)$ could be measured at various vertical distances z away from the upper (cold) plate. All the movable thermistors used in the experiment were calibrated individually with an accuracy 0.01 °C. A Keithley multimeter was used to measure the resistance of the thermistor at a sampling rate of 20 Hz. The frequency power spectrum $P(f)$ was computed using a LABVIEW fast Fourier transform (FFT) program provided by National Instruments. Typically, 1024 data points were used in the FFT and the result was averaged over an 8.3-h-long time record.

III. RESULTS AND DISCUSSION

A. Temperature statistics

We first discuss the local temperature measurements at the center of the smooth and rough cells with aspect ratio $A=1$. The measured $T(t)$ in both cells shows intermittent sharp spikes of variable heights and more fluctuations are found in the rough cell. Figure 1 compares the temperature histograms $H(\delta T)$ obtained in the rough cell (triangles) and in the smooth cell (solid curve). Here δT is defined as $T-\overline{T}$, with $\overline{T}$ being the local mean temperature. The measured $H(\delta T)$ in the smooth cell has a simple exponential form over an amplitude range of more than four decades. This exponential form has been observed previously in low-temperature helium gas [2]. It is seen from Fig. 1 that the measured $H(\delta T)$ in the rough cell is of the same exponential form as that in the smooth cell but has a larger rms value $\sigma=\langle(T-\overline{T})^2\rangle^{1/2}$. This suggests that temperature fluctuations in the rough cell are increased considerably when compared with those in the smooth cell.

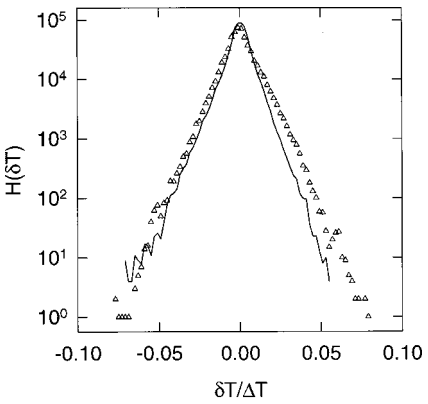

FIG. 1. Comparison of the temperature histograms $H(\delta T)$ obtained in the $A=1$ smooth cell (solid curve) and in the $A=1$ rough cell (triangles). The measurements were made at $\mathrm{Ra}=2.3\times10^9$ in the smooth cell and at $\mathrm{Ra}=2.1\times10^9$ in the rough cell.

Figure 2 shows the measured $H(\delta T)$ as a function of

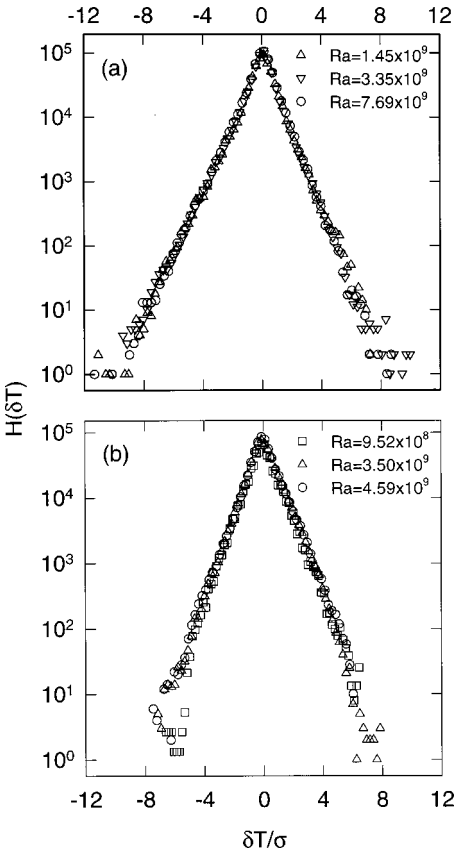

FIG. 2. Measured temperature histogram $H(\delta T)$ as a function of $\delta T/\sigma$ for three different values of Ra at the center of (a) the $A=1$ smooth cell and (b) the $A=1$ rough cell.

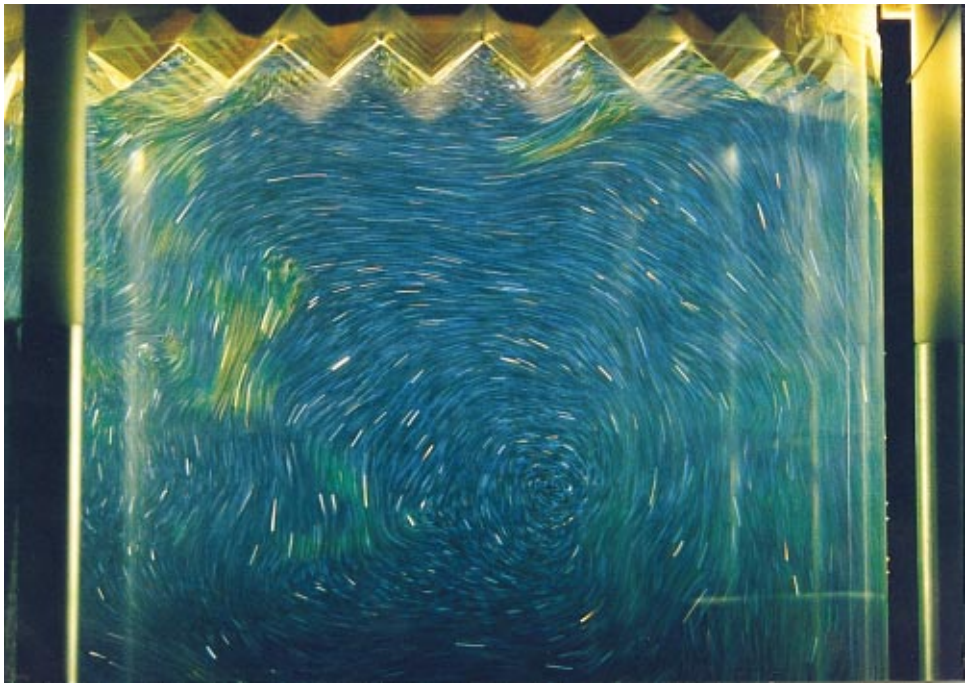

FIG. 3. (Color) A streak picture of the TLC spheres taken in the $A=1$ rough cell at Ra$=2.6\times10^9$. Cold eruptions are brown; green and blue regions are warmer. The displayed region covers the top 2/3 of the convection cell and its dimension is approximately 20×14 cm^2.

$\delta T/\sigma$ for three different values of Ra at the center of the $A=1$ smooth cell [Fig. 2(a)] and the $A=1$ rough cell [Fig. 2(b)]. It is seen that the measured $H(\delta T)$ for different values of Ra can all be brought into coincidence, once δT is scaled by its rms value σ. Plots of $H(\delta T)$ vs $\delta T/\sigma$ remain invariant and only σ changes with Ra. Over an amplitude range of almost five decades, all the temperature histograms exhibit the same exponential shape. The normalized width $\sigma/\Delta T$ of the distribution function is found to decrease with increasing Ra, indicating that the relative temperature fluctuations are reduced when the flow becomes more turbulent. Similar scaling behavior has been observed previously in a smooth cell by Castaing *et al.* [2]. The fact that the measured $H(\delta T)$ in the rough cell shows the same scaling behavior suggests that the temperature structure in the central region of the rough cell remains the same as that in the smooth cell and is invariant with Ra.

To visualize the temperature and velocity fields in the rough cell, we used a photographic technique [17] to take streak pictures of small thermochromic liquid crystal (TLC) spheres seeded in the convecting fluid. These TLC spheres change color from red to blue over a temperature range of 4 °C (29–33 °C). In the experiment, a thin vertical sheet of white light was shone through a central section of the convection cell. Figure 3 shows an instantaneous flow field in the $A=1$ rough cell. A large-scale circulation of size comparable to the cell dimension is observed and the ''eye'' of the circulation is located approximately at the cell center.

Our recent velocity measurements [20] in the $A=1$ smooth cell have shown that velocity fluctuations in the central region are homogeneous and larger than the mean velocity. Despite the large velocity fluctuations, the flow field still maintains a coherent structure, which undergoes a quasi-two-dimensional rotation around the cell center. Near the boundary, the large-scale rotation is found to persist over a long period of time and its mean value becomes larger than the fluctuations. The present flow visualization and more recent velocity measurements near the rough surface [21] indicate that the large-scale flow structure in the rough cell is similar to that in the smooth cell.

It is seen from Fig. 3 that there are some small eddies trapped inside the grooves. Our recent near-wall temperature measurements [16,17] showed that the small eddies are generated by the interaction between the horizontal shear flow (due to the large-scale circulation) and the rough surface. These eddies together with the large-scale horizontal flow cause eruption of thermal plumes near the tips of the pyramids. Figure 3 shows a cold plume, which just erupted from the tip of the third pyramid (from the right). Because the eruption of thermal plumes over the rough surface is driven mainly by the large-scale flow, rather than by the buoyancy force, most thermal plumes in the rough cell lose their mushroom shape. The small eddies in the groove region have a strong mixing effect, which produces large temperature fluctuations. Consequently, the temperature statistics near the rough surface are very different from those near the smooth surface [17].

The temperature fluctuations in the $A=0.5$ cells show a similar scaling behavior to those in the $A=1$ cells. Figure 4 shows the measured $H(\delta T)$ as a function of $\delta T/\sigma$ for three different values of Ra at the center of the $A=0.5$ smooth cell [Fig. 4(a)] and the $A=0.5$ rough cell [Fig. 4(b)]. The measured histograms in both cells scale with $\delta T/\sigma$. However, the shape of the measured $H(\delta T)$ in the $A=0.5$ cells is no longer of simple exponential form.

Figure 5 shows the measured $H(\delta T)$ as a function of $(\delta T/\Delta T)^{1.5}$ in the $A=0.5$ rough cell (triangles) and in the $A=0.5$ smooth cell (solid curve). It is seen that over an amplitude range of almost five decades the measured temperature histograms in both the smooth and rough cells appear as straight lines, indicating that they have a common stretched exponential form $H(\delta T)=H_0\exp[-\kappa(\delta T/\Delta T)^{1.5}]$, where H_0

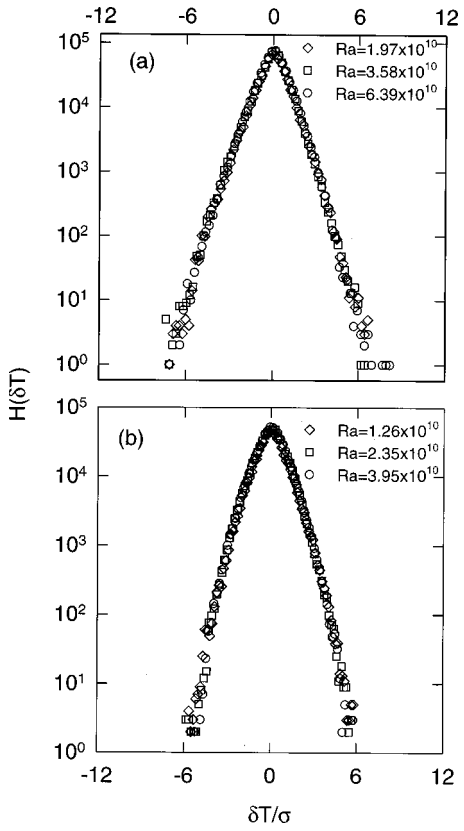

FIG. 4. Measured temperature histogram $H(\delta T)$ as a function of $\delta T/\sigma$ for three different values of Ra at the center of (a) the $A=0.5$ smooth cell and (b) the $A=0.5$ rough cell.

and κ are two fitting parameters. Figure 5 clearly shows that the measured $H(\delta T)$ in the rough cell has a larger rms value. It was suggested [22,23] that the shape change of the measured $H(\delta T)$ is caused by the fact that the large-scale circulation becomes unstable in the $A=0.5$ cell.

We now examine how σ changes with Ra. Figure 6(a) shows the measured $\sigma/\Delta T$ as a function of Ra at the center of the smooth cells (circles) and the rough cells (triangles). The measured $\sigma/\Delta T$ in both the $A=1$ and $A=0.5$ smooth

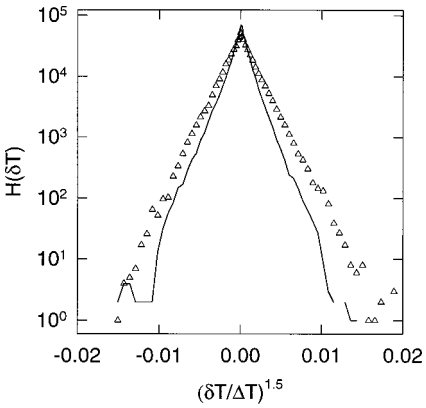

FIG. 5. Measured $H(\delta T)$ as a function of $(\delta T/\Delta T)^{1.5}$ in the $A=0.5$ smooth cell (solid curve) and in the $A=0.5$ rough cell (triangles). The measurements were made at $\mathrm{Ra}=2.8\times10^{10}$ in the smooth cell and at $\mathrm{Ra}=3.0\times10^{10}$ in the rough cell.

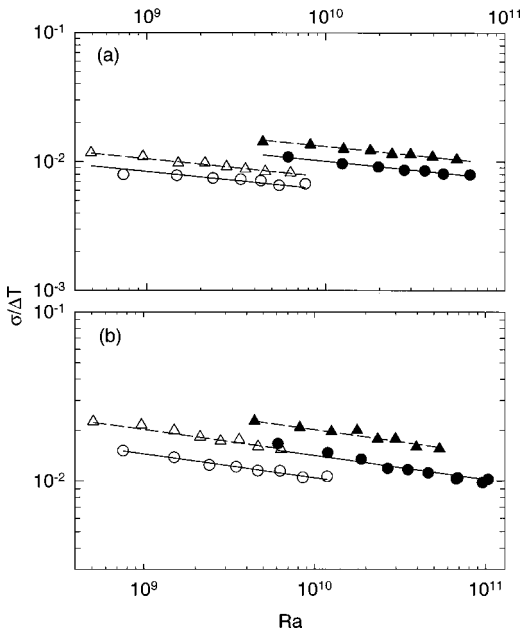

FIG. 6. Normalized rms value $\sigma/\Delta T$ as a function of Ra in the smooth cells (circles) and in the rough cells (triangles). The temperature measurements were conducted (a) at the cell center and (b) at a distance $z=2.4$ cm away from the upper (cold) surface. The closed symbols represent the data obtained from the $A=0.5$ cells and the open symbols are from the $A=1$ cells. The solid and dashed lines are the power-law fits to each set of data points.

cells is well described by the power law $\sigma/\Delta T=a\mathrm{Ra}^{-0.14}$ (solid lines). This scaling behavior agrees with the previous measurements in low-temperature helium gas [2,23]. Because of the larger temperature fluctuations, the power-law amplitude a in the $A=0.5$ cell is increased from 0.153 to 0.253. The measured $\sigma/\Delta T$ in the rough cells can also be described by a power law with the same exponent, but the value of a is changed from 0.153 to 0.192 in the $A=1$ cell and from 0.253 to 0.33 in the $A=0.5$ cell (dashed lines). The measured $\sigma/\Delta T$ in the rough cells is thus increased by 25–30 %, even at the cell center far away from the rough surfaces.

Similar scaling behavior is also observed at other locations in the bulk region. Figure 6(b) shows the measured $\sigma/\Delta T$ as a function of Ra, when the movable thermistor is placed at a distance $z=2.4$ cm away from the upper surface. The solid and dashed lines are the power-law fits to each set of data points. The fitted functions are $\sigma/\Delta T=0.28\mathrm{Ra}^{-1/7}$ (left solid line), $0.38\mathrm{Ra}^{-1/7}$ (right solid line), $0.39\mathrm{Ra}^{-1/7}$ (left dashed line), and $0.54\mathrm{Ra}^{-1/7}$ (right dashed line). Figure 6 thus demonstrates that the normalized rms values $\sigma/\Delta T$ in different cells and at various locations far away from the rough surface can all be described by power laws of Ra with a common exponent close to 1/7, but the power-law amplitudes vary with the spatial location and the aspect ratio of the cell.

B. Frequency power spectrum

Figure 7(a) shows the measured temperature power spectrum $P(f)$ as a function of f for three different values of Ra

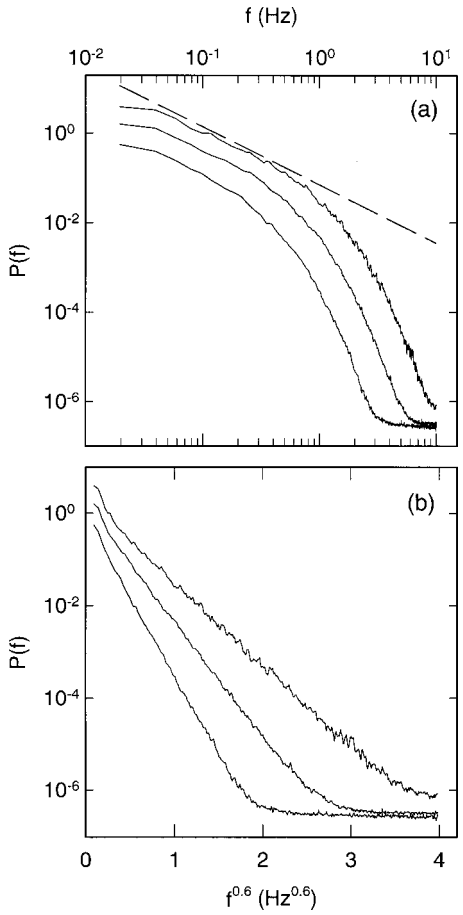

FIG. 7. (a) Measured temperature power spectrum $P(f)$ as a function of f for three different values of Ra at the center of the $A=1$ rough cell. The values of Ra are 9.5×10^8 (bottom curve), 2.1×10^9 (middle curve), and 4.6×10^9 (top curve). The dashed line indicates the power law $P(f)\sim f^{-1.3}$. (b) Plots of $P(f)$ as a function of $f^{0.6}$ for the same data sets.

at the center of the $A=1$ rough cell. Previous low-temperature measurements in the smooth cell [24] showed that the low-frequency portion of $P(f)$ can be described by a power law $P(f)\sim f^{-\alpha}$ with $\alpha\simeq 7/5$. This value of α was first predicted for the energy cascade in turbulence with thermal stratification [25–27]. However, Siggia [1] pointed out recently that similar scaling exponents were also observed for a passive scalar behind a cylinder and in a turbulent boundary layer. The dashed line in Fig. 7(a) indicates the power law $P(f)\sim f^{-1.3}$. Because of the limited range of f, the fitted values of α vary between 1.2 and 1.4 in our working range of Ra.

At higher frequencies, the measured $P(f)$ drops sharply and can be fitted by a stretched exponential function $P(f)\sim\exp[-(f/f_c)^{0.6}]$, where f_c is a cutoff frequency. Figure 7(b) shows the semilogarithmic plot of the measured $P(f)$ as a function of $f^{0.6}$ for three different values of Ra. In this plot, the stretched exponential function appears as a straight line. This form of $P(f)$ has been observed previously in a smooth cell by Wu *et al.* [22,24]. We also measured $P(f)$ in the $A=0.5$ rough cell at various values of Ra. The measured $P(f)$ shows a similar behavior to that in the $A=1$ rough cell.

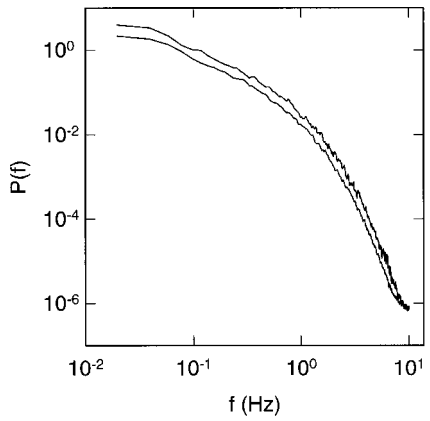

FIG. 8. Comparison of the temperature power spectra obtained in the $A=1$ smooth cell (lower curve) and in the $A=1$ rough cell (upper curve). The measurements were made at $\mathrm{Ra}=2.3\times10^9$ in the smooth cell and at $\mathrm{Ra}=2.1\times10^9$ in the rough cell.

Figure 8 compares the measured $P(f)$ in the $A=1$ rough cell (upper curve) and in the $A=1$ smooth cell (lower curve). It is seen that the measured $P(f)$ in the rough cell is of the same shape as that in the smooth cell but has a larger amplitude. This suggests that temperature fluctuations in the rough cell are increased uniformly across the whole frequency range. Note that $P(f)$ is related to the rms value σ via $\sigma^2=\int_0^{+\infty}P(f)df$.

C. Thermal dissipation

Clearly, the sharp decay of $P(f)$ at high frequency is caused by the dissipation in turbulent convection. The cutoff frequency f_c, therefore, becomes a measure of the thermal dissipation in the system. We now discuss the Ra dependence of f_c and its physical significance. The value of f_c was obtained from the slope of the straight lines shown in Fig. 7(b). Figure 9 shows the normalized f_c as a function of Ra in the smooth cells (circles) and in the rough cells (triangles). In the plot, f_c is normalized by the thermal diffusion time H^2/χ. It is seen that the measured f_cH^2/χ in the smooth and

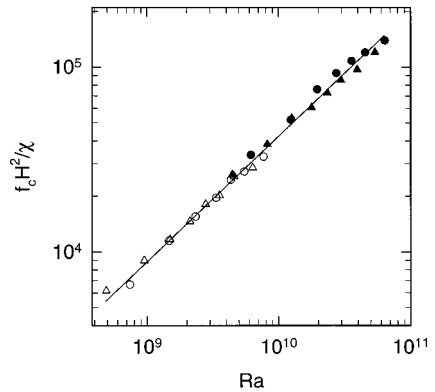

FIG. 9. Normalized cutoff frequency f_cH^2/χ as a function of Ra in the smooth cells (circles) and in the rough cells (triangles). The closed symbols represent the data obtained from the $A=0.5$ cells, and the open symbols are from the $A=1$ cells. The solid line shows the power-law fit $f_cH^2/\chi=6.7\times10^{-3}\mathrm{Ra}^{0.68}$.

rough cells with different aspect ratios can all be superposed onto a single master curve, indicating that the thermal dissipation in these cells is determined by the same mechanism. The measured $f_c H^2/\chi$ is found to be well described by the power law $f_c H^2/\chi = 6.7\times 10^{-3}\mathrm{Ra}^{0.68}$ (solid line).

The cutoff frequency f_c has been measured previously in a smooth cell filled with mercury [13,28], compressed gases [29], and low-temperature helium gas [22,27,30]. In these experiments, f_c was obtained using different cutoff functions for $P(f)$. In the present experiment and the early low-temperature experiment [22,24], the high-frequency cutoff of $P(f)$ is fitted to a stretched exponential function. With this fitting one obtains f_c, which is independent of the low-frequency behavior of $P(f)$. The helium data were also analyzed with a classical exponential cutoff multiplied by a power law for the low-frequency portion of $P(f)$ [24,27,30]. The fitted f_c is found to have the same Ra dependence as that obtained with the stretched exponential cutoff, but its magnitude is increased by a factor of 3.3 [22,24]. In the experiment with compressed gases [29], f_c was defined simply as the frequency at which the power spectrum intersects the noise level of the measurement. As shown in Fig. 7, the cutoff frequency defined in this way is approximately 80 times larger than that with the stretched exponential cutoff.

The measured f_c is found to be well described by a power law $f_c \sim \mathrm{Ra}^{\xi}$, but the exponent ξ varies with the convecting fluids used in the experiment. In helium gas (Pr$\simeq$0.7), one finds $\xi \simeq 0.78$ both at the cell center [22,27,30] and near the boundary [29]. In mercury (Pr=0.024), however, one gets $\xi \simeq 0.4$ [13]. The value of ξ obtained in water (Pr=5.4) is 0.68, which is between the other two values. These measurements indicate that ξ depends on the Prandtl number Pr.

It was suggested [13,27,29] that the cutoff frequency is given by $f_c = u_c/\ell_c$, where ℓ_c and u_c are, respectively, the characteristic length and velocity in turbulent convection. If the thermal boundary layer thickness [29] $\delta \simeq H/(2\mathrm{Nu})$ is taken as ℓ_c and the rms velocity [31] $v_0 \simeq 2.2\times 10^{-5}\mathrm{Ra}^{3/7}$ cm/s at the cell center is used as u_c, we have

$$\frac{f_c H^2}{\chi} \simeq 0.026\mathrm{Ra}^{5/7}. \tag{1}$$

In the above, we have used our recent heat transport result [17] $\mathrm{Nu}\simeq 0.17\mathrm{Ra}^{2/7}$. The calculated exponent in Eq. (1) is very close to the measured ξ and the power-law amplitude is of the same order of magnitude as the measured value. As discussed above, the exact numerical value of f_c may vary depending on how it is extracted.

To further verify that the thermal boundary layer thickness δ is the correct length scale for the above argument, we measured the velocity power spectrum $V(f)$. It is found [20] that $V(f)$ decays much faster than does the corresponding $P(f)$. Consequently, the measured $V(f)$ has a smaller cutoff frequency. This suggests that the length scale that controls the decay of $V(f)$ is larger than that for $P(f)$. Because the Prandtl number of water is 5.4, one expects the Kolmogorov viscous dissipation length [32] η to be larger than δ. We therefore conclude that the decay of $P(f)$ in water is determined by δ, whereas the decay of $V(f)$ is controlled by η.

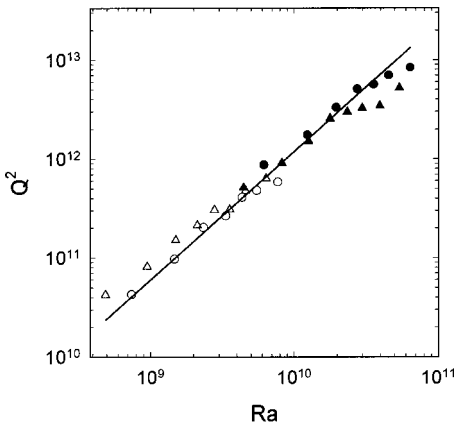

FIG. 10. Measured Q^2 as a function of Ra at the center of the smooth cells (circles) and the rough cells (triangles). The closed symbols represent the data obtained from the $A=0.5$ cells and the open symbols are from the $A=1$ cells. The solid line is a power-law fit to the circles.

Another quantity related to the thermal dissipation is $\langle(\partial T/\partial t)^2\rangle$, which has been called the ''dissipative power'' [27]. From the time series data, we have $\partial T/\partial t \simeq [T(t+\tau) - T(t)]/\tau$, where $\tau = 0.05$ s is the sampling time used in the local temperature measurements. This time is much smaller than the decay time $1/f_c$ of $P(f)$. Figure 10 shows the normalized quantity $Q^2 = \langle(\partial T/\partial t)^2\rangle H^4/(\sigma\chi)^2$ as a function of Ra at the center of the smooth cells (circles) and the rough cells (triangles). Within the experimental uncertainties, the measured Q^2 in the smooth and rough cells with different aspect ratios can all be superposed onto a single curve. This feature further confirms that the thermal dissipation in these cells is controlled by the same mechanism. The solid line in Fig. 10 shows the fitted power law $Q^2 = 0.12\mathrm{Ra}^{1.3}$ to the smooth cell data (circles).

The quantity Q^2 has been measured previously in helium gas [22,27]. The power-law exponent obtained for Q^2 is 1.34 ± 0.04, which agrees with our value in water. Procaccia *et al.* [27] proposed a scaling argument to explain the power-law exponent for Q^2. They argued that $\langle(\partial T/\partial t)^2\rangle \simeq u_c^2\langle(\nabla T)^2\rangle$ and thus $Q^2 \simeq (u_c H/\chi)^2(\Delta T/\sigma)^2\mathrm{Nu}$. With the experimental results: $u_c H/\chi = 0.3\mathrm{Ra}^{0.44}$ [31], $\mathrm{Nu} = 0.17\mathrm{Ra}^{0.29}$ [17], and $\sigma/\Delta T = 0.15\mathrm{Ra}^{-0.14}$ (see Fig. 6), we find $Q^2 = 0.68\mathrm{Ra}^{1.45}$. This calculation gives an upper bound for the measured Q^2 in Fig. 10.

IV. CONCLUSION

We have carried out a systematic study of temperature fluctuations in turbulent thermal convection. The experiment is conducted in a convection cell with rough upper and lower surfaces. Temperature statistics, frequency power spectrum, and thermal dissipation are measured over varying Rayleigh numbers in the central region of the cell. The results in the rough cell are compared with those in a smooth cell.

From these measurements at the cell center and the earlier temperature measurements near the rough surface [16,17], we conclude that the main effect of the surface roughness is to increase the emission frequency of the thermal plumes near the tip of the rough elements. These extra thermal plumes enhance the heat transport in the rough cell. While the surface roughness strongly alters temperature fluctuations near the rough surface, the basic temperature statistics as well as the thermal dissipation in the central region far away from the rough surface remain unchanged. The temperature histogram in the $A=1$ rough cell is found to have the same exponential shape as that in the smooth cell. The width of the distribution function (i.e., the normalized rms value $\sigma/\Delta T$) obeys a power law of Ra with the same exponent as that in the smooth cell. The power-law amplitude, however, is increased by $\sim$25% due to the enhancement of plume emission. The measured power spectrum shows that temperature fluctuations in the rough cell are increased uniformly across the whole frequency range.

The experiment indicates that the temperature statistics in the central region are determined primarily by turbulent mixing, which is controlled by the velocity fluctuations and is not sensitive to the detailed emission dynamics of the thermal plumes near the boundary. The complexity of the system comes from the interaction between the large-scale flow and the thermal plumes. Our recent velocity measurements [20] revealed that the large-scale circulation is driven by spatially separated rising and falling thermal plumes near the sidewall. The central region of the cell is ''sheared'' by the rising and falling flows near the sidewall and remains passive with a constant mean velocity gradient. Clearly, direct measurements of the velocity-temperature correlation are needed in order to further understand the mixing dynamics in turbulent convection.

ACKNOWLEDGMENTS

We thank X.-L. Qiu for his contributions in the velocity measurement and M. Lucas and his team for fabricating the convection cells. This work was supported by the National Science Foundation under Grant No. DMR-9623612.

[1] E. D. Siggia, Annu. Rev. Fluid Mech. **26**, 137 (1994).
[2] B. Castaing *et al.*, J. Fluid Mech. **204**, 1 (1989).
[3] B. I. Shraiman and E. D. Siggia, Phys. Rev. A **42**, 3650 (1990).
[4] S. Grossmann and D. Lohse, J. Fluid Mech. **407**, 27 (2000).
[5] F. Heslot, B. Castaing, and A. Libchaber, Phys. Rev. A **36**, 5870 (1987).
[6] R. H. Kraichnan, Phys. Fluids **5**, 1374 (1962).
[7] T. H. Solomon and J. P. Gollub, Phys. Rev. Lett. **64**, 2382 (1990); Phys. Rev. A **43**, 6683 (1991).
[8] Y.-M. Liu and R. E. Ecke, Phys. Rev. Lett. **79**, 2257 (1997).
[9] J. J. Niemela, L. Skrbek, K. R. Sreenivasan, and R. J. Donnelly, Nature (London) **404**, 837 (2000).
[10] S. Ciliberto, S. Cioni, and C. Laroche, Phys. Rev. E **54**, R5901 (1996).
[11] K.-Q. Xia and S.-L. Lui, Phys. Rev. Lett. **79**, 5006 (1997).
[12] S. Cioni, S. Ciliberto, and J. Sommeria, J. Fluid Mech. **335**, 111 (1997).
[13] T. Takeshita, T. Segawa, J. G. Glazier, and M. Sano, Phys. Rev. Lett. **76**, 1465 (1996).
[14] J. A. Glazier, T. Segawa, A. Naert, and M. Sano, Nature (London) **398**, 307 (1999).
[15] X.-C. Xu, K. M. S. Bajaj, and G. Ahlers, Phys. Rev. Lett. **84**, 4357 (2000).
[16] Y.-B. Du and P. Tong, Phys. Rev. Lett. **81**, 987 (1998).
[17] Y.-B. Du and P. Tong, J. Fluid Mech. **407**, 57 (2000).
[18] M. R. Raupach, R. A. Antonia, and S. Rajagopalan, Appl. Mech. Rev. **44**, 1 (1991).
[19] H. Tennekes and J. L. Lumley, *A First Course in Turbulence* (MIT Press, Cambridge, MA, 1972).
[20] X.-L. Qiu, S.-H. Yao, and P. Tong, Phys. Rev. E **61**, R6075 (2000).
[21] X.-L. Qiu, K.-Q. Xia, and P. Tong (unpublished).
[22] X.-Z. Wu, Ph.D. thesis, University of Chicago, 1991 (unpublished).
[23] X.-Z. Wu and A. Libchaber, Phys. Rev. A **45**, 842 (1992).
[24] X.-Z. Wu, L. Kadanoff, A. Libchaber, and M. Sano, Phys. Rev. Lett. **64**, 2140 (1990).
[25] R. Bolgiano, J. Geophys. Res. **64**, 2226 (1959).
[26] A. M. Obukhov, Dokl. Akad. Nauk SSSR **125**, 1246 (1959) [Sov. Phys. Dokl. **4**, 61 (1959)].
[27] I. Procaccia, E. S. Ching, P. Constantin, L. Kadanoff, A. Libchaber, and X.-Z. Wu, Phys. Rev. A **44**, 8091 (1991).
[28] S. Cioni, S. Ciliberto, and J. Sommeria, Europhys. Lett. **32**, 413 (1995).
[29] A. Belmonte, A. Tilgner, and A. Libchaber, Phys. Rev. Lett. **70**, 4067 (1993); Phys. Rev. E **50**, 269 (1994).
[30] M. Sano, X.-Z. Wu, and A. Libchaber, Phys. Rev. A **40**, 6421 (1989).
[31] Y. Shen, K.-Q. Xia, and P. Tong, Phys. Rev. Lett. **75**, 437 (1995).
[32] U. Frisch, P. Sulem, and M. J. Nelkin, J. Fluid Mech. **87**, 719 (1978).